Multi-particle trapping and manipulation by a high-frequency array transducer

Changhan Yoon, Bong Jin Kang, Changyang Lee, Hyung Ham Kim,[a] and K. Kirk Shung
NIH Resource Center for Medical Ultrasonic Transducer Technology and Department of Biomedical Engineering, University of Southern California, Los Angeles, California 90089, USA

(Received 24 September 2014; accepted 16 November 2014; published online 24 November 2014)

We report the multiple micro-particle trapping and manipulation by a single-beam acoustic tweezer using a high-frequency array transducer. A single acoustic beam generated by a 30 MHz ultrasonic linear array transducer can entrap and transport multiple micro-particles located at the main lobe and the grating lobes. The distance between trapped particles can be adjusted by changing the transmit arrangement of array-based acoustic tweezers and subsequently the location of grating lobes. The experiment results showed that the proposed method can trap and manipulate multiple particles within a range of hundreds of micrometers. Due to its simplicity and low acoustic power, which is critical to protect cells from any thermal and mechanical damages, the technique may be used for transportation of cells in cell biology, biosensors, and tissue engineering. © *2014 AIP Publishing LLC*. [http://dx.doi.org/10.1063/1.4902923]

Multi-trapping of cells and microparticles is of particular importance in many biological applications including cell biology, biosensors, and tissue engineering.[1–5] Various methods (e.g., optical tweezers, magnetic tweezers, standing surface waves based acoustic tweezers, and microstreaming) have been developed for simultaneously manipulating multiple cells/particles or arranging them into desired patterns.[6–10] Among them, the acoustic tweezers have several advantages in miniaturization, low power consumption, and technical simplicity.[8] Acoustic vortices, in which particles more than 0.6 λ (λ is the wavelength) apart can be captured and manipulated within a region of 1.6 λ, have recently developed.[10] The method utilized a ring-shape array transducer to form Bessel beams by precisely controlling amplitude and phase delay at each element. Unlike the standing wave based acoustic tweezers that use a pair of transducers in a parallel or orthogonal arrangement,[8–10] a single-beam acoustic tweezer of which trapping mechanism is similar to that of the optical tweezers utilized a single element or an array ultrasonic transducer to trap and manipulate a single cell and microparticle.[11–13] Since the acoustic tweezers use output power of diagnostic range, there are no thermal and mechanical effects produced on cells, which are critical in biological studies.[8,12,14]

In this paper, we report the feasibility of multi-particle trapping with a single-beam acoustic tweezer using a high-frequency array transducer. In the method, a sparse array (SA) that utilized partial elements in a fully sampled array (FSA) for transmission is applied to separate the microparticles into desired positions. In fact, the SA method was proposed to reduce the number of active elements that are directly related to the hardware complexity while preserving the lateral resolution in medical ultrasound imaging.[15,16]

Figure 1 shows the general model of periodic SA arrangement. It is arranged to have N sub-apertures, where each sub-aperture is formed by S elements (S is defined as sparse factor) with R consecutive elements (R is the repetition factor, $S \geq R$) that are actually used for transmitting. Note that the elements shaded in gray are used for transmission in the SA as shown in Fig. 1. When $S = R$, it becomes a FSA that is typically used in the medical ultrasound imaging. From the geometry of transducer, the transmitting focus time delay of i_{th} element (τ_i) for a focal point at (x_f, z_f) can be calculated by

$$\tau_i = \frac{1}{c}\left(\sqrt{(x_f - x_i)^2 + z_f^2} - z_f\right), \tag{1}$$

where c is the sound speed and x_i is the distance from the center of array to i_{th} element, respectively. By using the Rayleigh diffraction formula with the Fresnel approximation, the transmit lateral beam pattern is expressed by[16]

$$\psi = \operatorname{sinc}\left(d\frac{u}{\lambda}\right) \cdot \frac{\sin\left(\pi NSd(u-u')/\lambda\right)}{\sin\left(\pi Sd(u-u')/\lambda\right)} \times \frac{\sin\left(\pi Rd(u-u')/\lambda\right)}{\sin\left(\pi d(u-u')/\lambda\right)}, \tag{2}$$

where d is the element pitch, $u = x/z_f = \sin\theta$ (θ: azimuth angle) and $u' = x_f/z_f = \sin\theta_0$ (θ_0: steering angle), respectively.

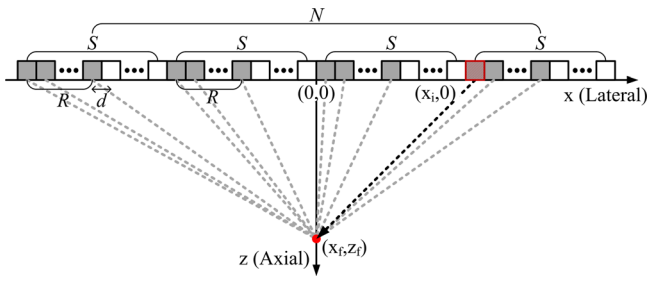

FIG. 1. General model of periodic SA arrangement. The array is arranged to have N sub-apertures, where each sub-aperture is formed by S elements with R consecutive elements that are actually used for transmitting ($S \geq R$).

[a]Author to whom correspondence should be addressed. Electronic mail: hyunghak@usc.edu. Tel.: +1-213-821-2647. Fax: +1-213-821-3897

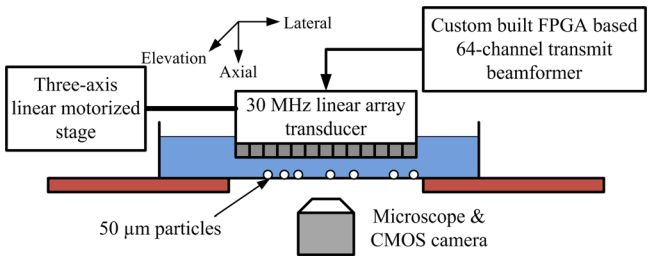

FIG. 2. Experiment setup of an array transducer based trapping.

From Eq. (2), the main lobe width is given by $2F\lambda/NSd$ (where k is the wave number and F is the transmit focal depth) and the grating lobes are appeared at $x = mF\lambda/Sd$ (m = integer) when a beam is not steered, i.e, $\theta_0 = 0$. In the periodic SA, the main lobe width that is important for high trapping force is maintained compared to that of FSA, and the locations of grating lobe can be adjusted by changing the sparse factor, i.e., S. Note that the grating lobes in the FSA are supressed by the first term in Eq. (2) (i.e., $\mathrm{sinc}(du/\lambda)$, directivity pattern of element) when the element pitch is equal to λ,[17] thus its trapping force is insufficient to capture a particle.

To assess the feasibilty of this approach, a high-frequency linear array fabricated with an interdigitally bonded 2–2 piezo-composite was utilized.[18] The 30-MHz array transducer has a 50 μm azimuth pitch (i.e., λ in water), and 2 mm elevation height with an acoustic lens for fixed elevation focusing at 7.3 mm. The transmit focusing using the delay law in the azimuth direction is electronically controlled by a custom built field programmable gate array (FPGA) based 64-channel ultrasound imaging system.[19] The system can transmit 64 bi-polar pulse upto 40 V_{pp} and the different transmit patterns can be configured by loading a look-up-table into the system. The array transducer was mounted on an inverted microscope (Olympus IX-71, Center Valley, PA) and the images were recorded using a high-sensitive CCD camera (ORCA-Flash2.8, Hamamatsu, Japan), as shown in Fig. 2. A three-axis linear motorized stage was used to position the transducer. Polystyrene microparticles with a mean diameter of 50 μm were suspended in a water chamber and the transducer excited sinusoidal burst from above. The reflection from the bottom of chamber does not appear to affect the trapping performance to any significant degree. This was demosntrated when a plastic bottom was replaced by a mylar membrane.[20]

The experiments were conducted with three different transmit configurations, i.e., FSA that use all 64 elements, and two SA patterns. The SA patterns were $S = 3$ and $R = 1$ (i.e., SA100) and $S = 4$ and $R = 2$ (i.e., SA1100), respectively.

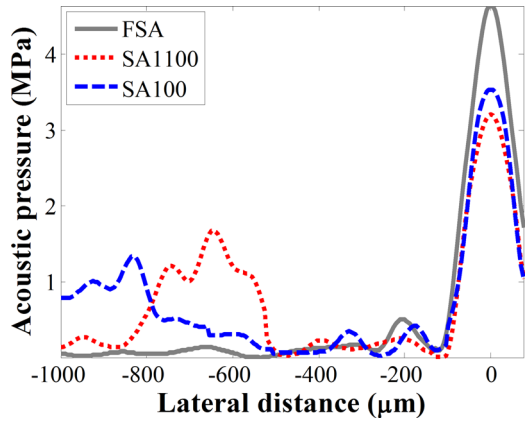

FIG. 3. Lateral acoustic pressures at focal depth from FSA, sparse arrays with $S = 3$ and $R = 1$ (i.e., SA100) and $S = 4$ and $R = 2$ (i.e., SA1100), respectively.

The electronical transmit focusing in the azimuth direction was achieved at a depth of 2.6 mm for tight focusing to attain higher trapping force. The excitation voltage for FSA was 30 V_{pp}, whereas it was 40 V_{pp} for both SA. A 200-cycles of 30 MHz sinusoidal burst was transmitted at a pulse repetition period of 1 ms (a duty factor of 0.67%).

The lateral acoustic pressures of FSA, SA100, and SA1100 were measured by a hydrophone (HPM04/01, Precision Acoustics, UK) and plotted in Fig. 3. The main lobe widths at −3 dB, acoustic pressures at main and grating lobes, and locations of first grating lobes are summarized in Table I. As listed in Table I, −3-dB beam widths of the main lobe produced by the SA1100 and SA100 patterns were comparable to the main lobe width of FSA. First grating lobes appeared at 650 μm and 830 μm for SA1100 and SA100, respectively. The magnitudes of the grating lobes in the SA methods were lower than that of the main lobe due to the directivity pattern of element.

Figure 4 shows the experiment results of FSA. A single microparticle indicated with an arrow was trapped and moved in the lateral direction by mechanically translating the array with the linear motorized stage. The SA1100 pattern produced the grating lobe at 650 μm was examined, which is shown in Fig. 5. Two microparticles apart from 650 μm (indicated with arrows) were simultaneously captured and moved as the transducer shifted. Note that SA pattern can trap and move two microparticles at the same time, whereas FSA can do a single microparticle only. Also note that only two particles trapped at the locations of the main and first grating lobes are shown in figures due to the limited field of view of the current microscope system, i.e., 1150 μm. It was also able to accomplish the different trapping position with SA100 of which grating lobe appeared at

TABLE I. Measured beam width at −3 dB and acoustic pressures at main and grating lobes, and locations of first grating lobe.

	Width (μm)		Acoustic pressure (MPa)		
	Main lobe	Grating lobe	Main lobe	Grating lobe	Location of first grating lobe (μm)
FSA	90	…	4.64	…	…
SA1100	92	95	3.21	1.68	650
SA100	96	84	3.54	1.34	830

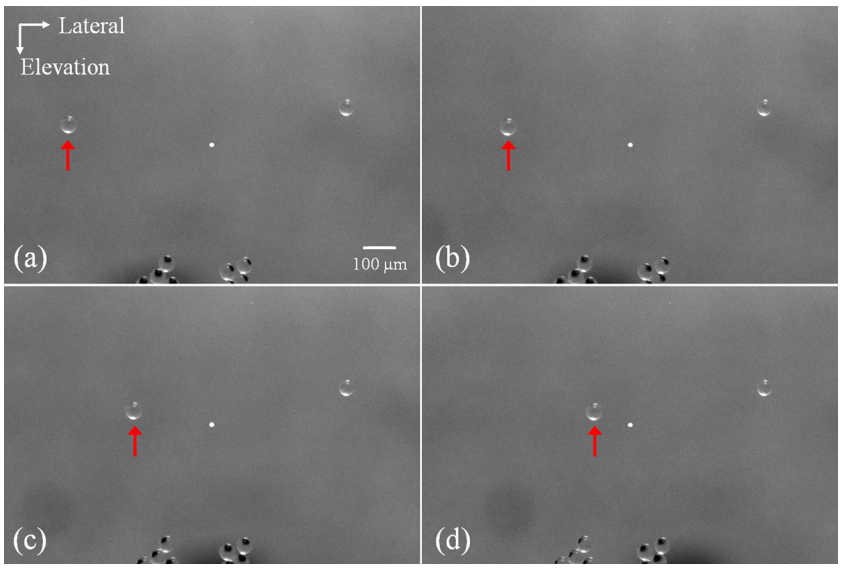

FIG. 4. (a) Single microparticle trapped and (b)–(d) manipulated by a FSA in the lateral direction. (Multimedia view) [URL: http://dx.doi.org/10.1063/1.4902923.1]

830 μm (see Fig. 6). The distance between two microparticles was measured to be 850 μm, which was within the 3 dB grating lobe width, i.e., 95 μm in this case. Since the transducer used in the experiments was fabricated for imaging purpose (elevation focal depth of 7.3 mm), it yielded broad beam pattern at 2.6 mm, resulting misaligned trapping position in the elevation direction, as shown in Fig. 6. Using a tightly focused transducer in the elevation direction, i.e., thinner slice of the beam, more precise positioning of particles would be possible. Also, a two-dimensional high-frequency array transducer will enable us to trap in a square-shape pattern and manipulate microparticles in both lateral and elevation directions.

The experiment results demonstrated that the high-frequency array transducer is capable of trapping not only a single microparticle but also multiple particles by adjusting the SA arrangements. The finding is in good agreement with the ray acoustic model which shows that the trapping force depends on intensity difference of incident beams at the interface, i.e., intensity gradient.[11] The experimental results showed that the gradient of acoustic intensity is sufficient to trap particles not only by the main lobe but also by the grating lobes that produce lower acoustic pressure. Pressure gradient was 54.4 MPa/mm for the main lobe, and those of the grating lobes for the SA100 and SA1100 were, respectively, 17.8 and 19.8 MPa/mm, indicating that the trapping force was resulted from the steep gradients, not from peak pressure itself. In these experiments, a spatial peak time averaged intensity value related to temperature increase was only 97.3 mW/cm^2 due to the low duty factor (0.67%). From the previous study,[14] it was reported that the temperature change was 1.6 °C when a spatial peak time averaged intensity was 477.8 mW/cm^2, thus the increase in temperature would be negligible in our experiments. The method does not require any additional treatments on the substrates or particles. These results indicated that the proposed method holds promise as a useful tool for biological applications, one of which is to interrogate cell to cell interaction. Heterotypic cell interaction between parenchymal cells and nonparenchymal neighbors plays a critical role in modulation of cell growth, migration, and differentiation. This method can be utilized for seeding two cell types (e.g., hepatocytes and nonparenchymal cells) in a desired position rather than random cocultures, which allows for specifying cell density and

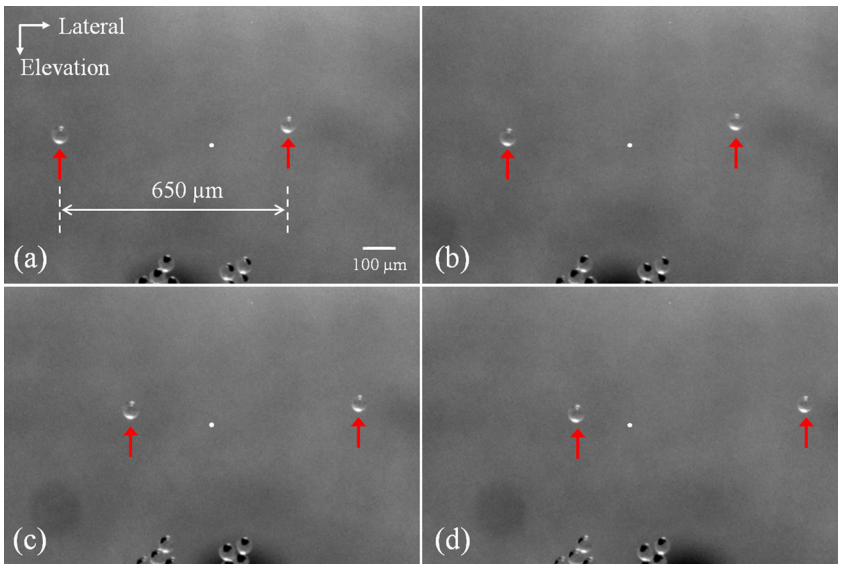

FIG. 5. (a) Microparticles trapped at the locations of the main lobe and grating lobe by a sparse array with $S = 4$ and $R = 2$ (SA1100) in the lateral direction, (b)–(d) moved with maintaining a distance between trapped particles. (Multimedia view) [URL: http://dx.doi.org/10.1063/1.4902923.2]

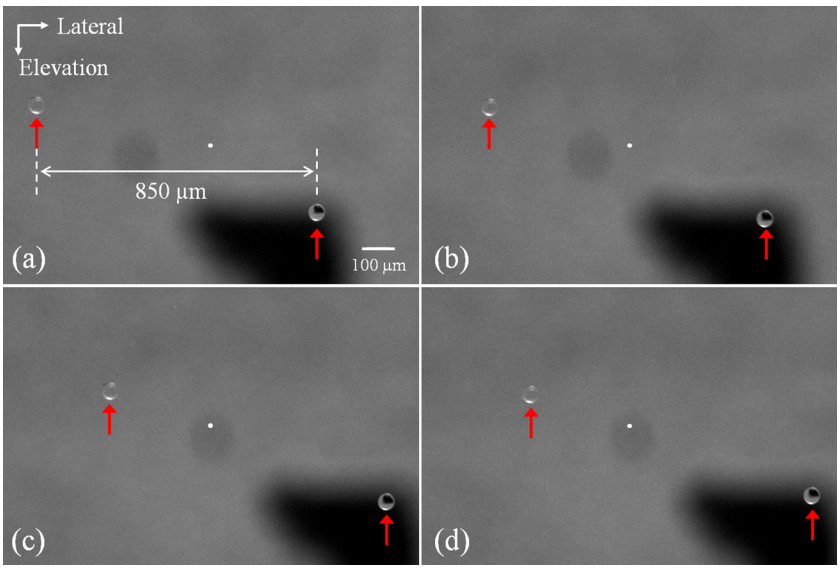

FIG. 6. (a) Microparticles trapped at the locations of the main lobe and grating lobe and (b)–(d) manipulated by a sparse array with $S = 3$ and $R = 1$ (SA100) in the lateral direction. Note that wide trapping zone was formed due to non-optimal focusing in the elevation direction. (Multimedia view) [URL: http://dx.doi.org/10.1063/1.4902923.3]

length of contact between the two cell populations.[21] In addition, it is expected to be useful in culturing cells on micro pH-sensor arrays to monitor and statistical analysis of cell metabolic activity.[22]

This work has been supported by the NIH Grants (No. R01-EB012058 and P41-EB002182).

[1]R. Singhvi, A. Kumar, G. P. Lopez, G. N. Stephanopoulos, D. I. C. Wang, G. M. Whitesides, and D. E. Ingber, Science **264**, 696 (1994).
[2]C. A. Thomas, P. A. Springer, G. E. Loeb, Y. Berwald-Netter, and L. M. Okun, Exp. Cell Res. **74**, 61 (1972).
[3]A. Folch and M. Toner, Annu. Rev. Biomed. Eng. **2**, 227 (2000).
[4]M. M. Stevens, M. Mayer, D. G. Anderson, D. B. Weibel, G. M. Whitesides, and R. Langer, Biomaterials **26**, 7636 (2005).
[5]C. J. Flaim, S. Chien, and S. N. Bhatia, Nat. Methods **2**(2), 119 (2005).
[6]A. Ashkin, J. M. Dziedzic, and T. Yamane, Nature **330**, 769 (1987).
[7]H. Lee, A. M. Purdon, and R. M. Westervelt, Appl. Phys. Lett. **85**(6), 1063 (2004).
[8]J. Shi, D. Ahmed, X. Mao, S. S. Lin, A. Lawit, and T. J. Huang, Lab Chip **9**, 2890 (2009).
[9]J. Zhang, L. Meng, F. Cai, H. Zheng, and C. R. P. Courtney, Appl. Phys. Lett. **104**, 224103 (2014).
[10]C. R. P. Courtney, C. E. M. Demore, H. Wu, A. Grinenko, P. D. Wilcox, S. Cochran, and B. W. Drinkwater, Appl. Phys. Lett. **104**, 154103 (2014).
[11]J. Lee, S. Teh, A. Lee, H. H. Kim, C. Lee, and K. Kirk. Shung, Appl. Phys. Lett. **95**, 073701 (2009).
[12]J. Lee, C. Lee, H. H. Kim, A. Jakob, R. Lemor, S. Teh, A. Lee, and K. Kirk Shung, Biotechnol. Bioeng. **108**(7), 1643 (2011).
[13]F. Zheng, Y. Li, H. Hsu, C. Liu, C. T. Chiu, C. Lee, H. H. Kim, and K. K. Shung, Appl. Phys. Lett. **101**, 214104 (2012).
[14]J. S. Jeong and J. Lee, J. Korean Phys. Soc. **62**(2), 238 (2013).
[15]G. R. Lockwood, P. Li, M. O'Donnell, and F. S. Foster, IEEE Trans. Ultrason. Ferroelect. Freq. Control **43**(1), 7 (1996).
[16]G. Kim and T.-K. Song, in *6th International Specialists Topic Conference on ITAB* (IEEE, 2007), p. 239.
[17]K. K. Shung and M. Zipparo, IEEE Eng. Med. Biol. Mag. **15**, 20 (1996).
[18]J. M. Cannata, J. A. Williams, L. Zhang, C. Hu, and K. K. Shung, IEEE Trans. Ultrason. Ferroelect. Freq. Control **58**(10), 2202 (2011).
[19]C. Hu, L. Zhang, J. M. Cannata, J. Yen, and K. K. Shung, Ultrasonics **51**(8), 953 (2011).
[20]J. Lee, C. Lee, and K. K. Shung, IEEE Trans. Ultrason. Ferroelect. Freq. Control **57**(10), 2305 (2010).
[21]S. N. Bhatia, U. J. Balis, M. L. Yarmush, and M. Toner, FASEB J. **13**, 1883 (1999).
[22]B. Nemeth, M. D. Symes, A. G. Boulay, C. Busche, G. J. T. Cooper, D. R. S. Cumming, and L. Cronin, Adv. Mater. **24**, 1238 (2012).